



# SPEI-based analysis of spatio-temporal variation characteristics for annual and seasonal drought in the Zoige Wetland, Southwest China from 1961 to 2016

Xiaoyan Jin<sup>1</sup> · Haofan Qiang<sup>2</sup> · Lu Zhao<sup>1</sup> · Shouzheng Jiang<sup>1</sup> · Ningbo Cui<sup>1</sup> · Yi Cao<sup>1</sup> · Yi Feng<sup>1</sup>

Received: 26 January 2019 / Accepted: 19 August 2019 / Published online: 14 September 2019  
© Springer-Verlag GmbH Austria, part of Springer Nature 2019

## Abstract

Water scarcity has a destructive impact on the social and economic development around the world. The present study investigated the variations of drought conditions during 1961–2016 in the Zoige Wetland of Southwest China by adapting the Mann–Kendall (MK) analysis, the Theil–Sen slope estimator, continuous wavelet transforms (CWT), and the inverse distance weighting (IDW) algorithm. The partial correlation coefficient (PC) was also used to understand the causes of Standardized Precipitation Evapotranspiration Index (SPEI) characteristics from different climate factors. The results showed that the majority of the wetland had a drying trend with a  $-0.142/(10 \text{ years})$  rate of SPEI on annual scale, while a 2–8-year significant period was observed on both annual and seasonal scales. In spring, the wetland presented dryness and had a tendency of mitigation except for the northeastern area. In summer, the wetland mainly presented humidity, but it had a drying trend except for the southern area. In autumn, the overall wetland was humid with an abrupt change towards dryness occurring around 1983 and the whole wetland showed a manifest drying trend. In winter, most areas showed drought while the Jiuzhi County and part of the southern wetland had an alleviating trend of drought. The decrease of annual SPEI was primarily due to the decrease in precipitation, the mean temperature increase, and relative humidity decrease that offset the reversed impact of wind speed decrease and sunshine duration decrease. The change of SPEI on a seasonal scale was the consequence of the significant change in precipitation only in winter. The results of this study would be of use for understanding the characteristics of climate variation and water resources management across the Zoige Wetland in a changing environment.

✉ Ningbo Cui  
ningbocui@126.com

Xiaoyan Jin  
jinxiaoyan96@163.com

Haofan Qiang  
qianghaofan96@163.com

Lu Zhao  
luya1121@126.com

Shouzheng Jiang  
shouzhengjiang@sina.com

Yi Cao  
caoyi@scu.edu.cn

Yi Feng  
fengyscu@163.com

<sup>1</sup> College of Water Resource and Hydropower, Sichuan University, Chengdu 610065, Sichuan, China

<sup>2</sup> School of Economics, Fudan University, Shanghai 200433, Shanghai, China

## 1 Introduction

The fifth IPCC (2013) report pointed out that global warming has become an indisputable fact, which resulted in frequent climate anomalies. In the context of global warming, climate change may trigger a series of frequent extreme weather events, including droughts, heavy rains, and high temperatures (Min et al. 2011). Among the abovementioned, the drought frequently defined as the water deficit during a target period (Tömros and Menzel 2014) is considered to be one of the mainly natural reasons of agricultural, environmental, and socioeconomic damages (Lou et al. 2017; Yang et al. 2016; Liu et al. 2015). Droughts are generally considered in four major types: meteorological, agricultural, hydrological, and socioeconomic drought (Jiang et al. 2018; AMS 2004; Wilhite 2005; Li et al. 2015a, b): (1) Meteorological drought results from the reduction of precipitation in a region for a period of time; (2) Agricultural drought is a reference to a period of insufficient soil moisture, resulting in reduced crop yields and plant growth; (3) Hydrological drought is caused

by insufficient surface and underground water supply; (4) Socioeconomic drought is related to the deficiency of supply to meet the demand of certain economic products with the above three types of droughts. Among these types of droughts, the meteorological drought is more frequent and widespread than the other three types of drought, normally triggering other types of drought (WMO 2006). Therefore, meteorological drought monitoring is of great significance for preceding warning and risk management of water resources and agricultural production (Zhang and Jia 2013).

To precisely measure regional drought severity, scientists have proposed lots of quantitative definitions of drought and related indicators (Burke et al. 2006). Drought index is an indicator that quantifies drought levels by assimilation of data from one or more variables (such as precipitation and evapotranspiration) into a single value that are easier to use than the raw indicator data (Zargar et al. 2011), and choosing the appropriate drought index is the basis for studying regional drought climate (Zhan et al. 2013). Recently, meteorological drought indexes mostly used include Palmer Drought Severity Index (PDSI) (Palmer, 1965), Standardized Precipitation Index (SPI) (McKee et al. 1993), and Standardized Precipitation Evapotranspiration Index (SPEI) (Vicente-Serrano et al. 2010), in applications such as drought forecasting, announcing drought levels, contingency planning, and impact assessment. Among these indexes above, the Palmer Drought Severity Index (PDSI), which takes antecedent precipitation, moisture supply, and moisture demand into consideration, has been commonly used to quantify the dryness and wetness conditions (Li et al. 2015a, b). It has achieved great success in long-term drought monitoring, but it is not satisfactory for solving short-term drought and only works well in arid and semiarid regions (Yang et al. 2016). In order to solve the temporal scale imperfection in the PDSI, the Standardized Precipitation Index (SPI) was developed by precipitation probabilistic approach (McKee et al. 1993), which is considered to be a better indicator for requiring fewer parameters. However, the main reason why SPI was criticized was that its calculations only used precipitation data without taking evapotranspiration into account (Törnros and Menzel 2014).

To tackle the drawbacks of the indexes above, Vicente-Serrano et al. (2010) proposed the Standardized Precipitation Evapotranspiration Index (SPEI) to assess drought, which is regarded as a suitable substitute for SPI and PDSI (Li et al. 2015a, b). The SPEI is based on water balance and can be compared with the self-calibrated PDSI (sc-PDSI) (Vicente-Serrano et al. 2010). SPEI combines the advantages of PDSI and SPI, taking into account the effects of temperature and precipitation on drought, making up for the shortcomings of SPI not considering temperature, and having a simpler, multi-time, and multi-space advantage compared with PDSI (Liu et al. 2016a, b). Especially, SPEI is expert in detecting, monitoring, and exploring the effects of global warming on

drought conditions (Dubrovsky et al. 2009), and has good applicability in wet areas of China (Yang et al. 2017). Thus, the SPEI has been widely used and discussed in recent years. Chen and Sun (2015) used SPEI to detect changes in drought characteristics in China and reported that since the late 1990s, droughts had become more frequent and severe across China, especially in some regions of northern China (Chen and Sun 2015). Li et al. (2015a, b) found it effective to monitor the drought in Southwest China by applying SPEI and the mean indicator values on five different time scales (1, 3, 6, 12, and 24 month) all decreased significantly from 1982 to 2012. Yang et al. (2016) used SPEI to conclude that annual and seasonal drought in the Haihe River Basin was becoming serious and frequent from 1960 to 2010. Li et al. (2015a, b) found no statistical trend in the number of wet and dry events using SPEI in the Yarlung Zangbo River Basin, but the severity of dry episode exacerbated in terms of duration and magnitude.

Indeed, high-frequency severe drought is one of the most devastating natural disasters in China caused by monsoon climates and complex geographic landscapes (Li et al. 2017). The socioeconomic losses in this country caused by serious drought had increased significantly over the past half century (Xu et al. 2015). However, literature mentioned above focused on the whole Southwest China with no particular focus on climate change in key locales. As one of the most important and ecosystem-vulnerable regions in China, as the third pole of the world, the Qinghai–Tibetan Plateau plays a key role in climate change because it has critical influence on climate in other parts of Asia and elsewhere in the Northern Hemisphere (Ma et al. 2015). The impacts of climate change and human activities on wetlands have drawn attention of the international community (Woodward et al. 2014). The Zoige Wetland, the world's most widely distributed and highest lying plateau peatland, is located in the upper reaches of the Yellow River and the northeastern margin of Qinghai–Tibetan Plateau, which is an ideal natural laboratory for ecology and climate research. It is an important ecological function region of water resources protection and the water storage capacity of the upper reaches of the Yellow River is nearly 840 million cubic meters, which is an important habitat for the protection of wetland biodiversity (Bai et al. 2013). But the variation characteristics and causes of the seasonal drought conditions in the background of global warming have not been comprehensively studied yet. Therefore, the study on the varying drought conditions of the Zoige Wetland under climate change is important to the ecological environment protection and utilization of water resources in the upper reaches of the Yellow River.

In the past, the 12-month SPEI was used to analyze regional drought changes on interannual scale; however, the SPEI on seasonal scale used in this paper considers the combined effects of temperature, precipitation, and surface evaporation

potential on seasonal drought, and can relatively objectively characterize the trend of water deficit in the study area (Zhang et al. 2018). Though the SPEI takes into account the multi-scale advantages of SPI and the advantages of PDSI considering evapotranspiration, it was found in earlier studies that when the average monthly temperature was below 0 °C, the potential evapotranspiration calculated by the Thornthwaite method failed (Zhuang et al. 2013). Liu et al. found that the SPEI based on the Penman–Monteith method can describe the characteristics of drought variations more reasonably, which was also used in our study that contributes to the existing research literature (Liu et al. 2015). In addition, this paper conducts analysis based on meteorological station data while some recent studies used meteorological remote sensing data and grid methods to analyze regional drought changes, which can be one of the improved methods for our future research.

Based on the analyses above, this paper aims to research the features of the drought/wetness conditions by using SPEI in the Zoige Wetland to provide a scientific suggestion to the relief of drought catastrophe using the daily meteorological data of 19 meteorological stations from 1961 to 2016. The main parts of our paper can be summarized as follows: (1) to study the interannual variability of SPEI on both annual and seasonal scales for 56 years; (2) to analyze the periodic variations of SPEI on both annual and seasonal scales using the Morlet wavelet transform; (3) to study the spatial distribution of SPEI and its trend using IDW (Inverse Distance Weighting algorithm, a commonly used spatial interpolation method assuming that the sample values closer to the prediction

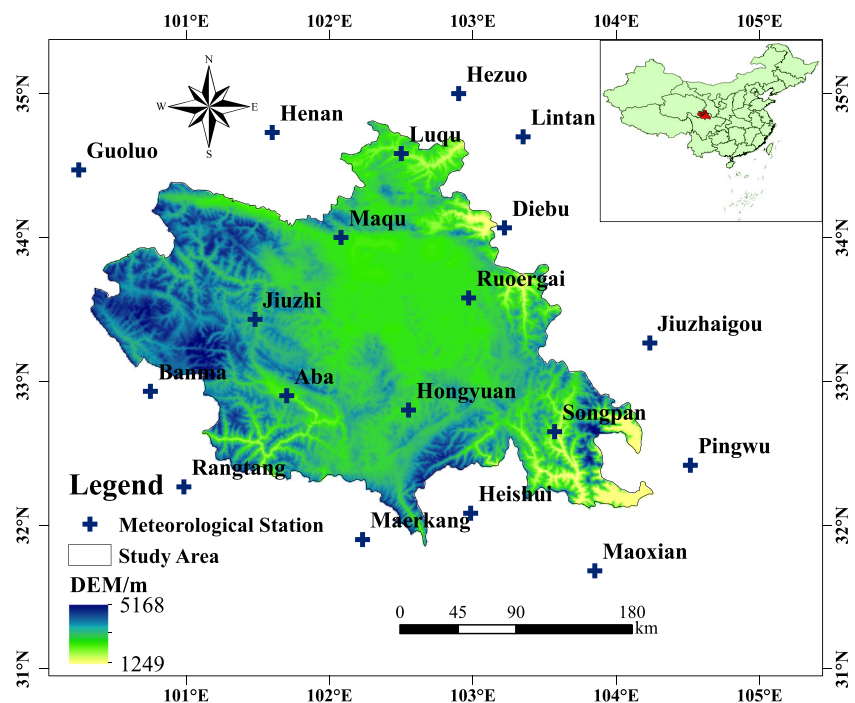
location are more representative than sample values farther away) on GIS; (4) to make attribution analysis of SPEI by partial correlation coefficients.

## 2 Materials and methods

### 2.1 Study area

The Zoige Wetland, one major swamp area in China, is located in the eastern part of the Qinghai–Tibetan Plateau with the average elevation of over 3700 m (Fig. 1). The wetland is considered as the kidney of the plateau for its significant ecological function of withholding water in the upper reaches of the Yellow River (Zhao et al. 2017a, b). The wetland covers approximately 16,000 km<sup>2</sup> (Li et al. 2014a). The area accounts for about one-third of the observed annual runoff of Maqu hydrological station in the Yellow River (4.6 billion m<sup>3</sup>) (Li et al. 2014a). Thus, the wetland plays a key role in biodiversity conservation and ecological security throughout Yellow River Basin (Zhao et al. 2017a, b). The Zoige Wetland includes the Ruoergai, Songpan, Hongyuan, and Aba counties in the northwestern part of Sichuan Province, the Maqu and Luqu counties in southwest Gansu Province, and the Jiuzhi County in southeast Qinghai Province. The climate of the study area is representative alpine humid and semi-humid continental monsoon with large differences in diurnal temperatures. There is a longer freezing season in the area, with an average annual temperature of about 0.6 to 1.2 °C and

**Fig. 1** Geographic locations of the meteorological stations and territory of the Zoige Wetland



an average annual precipitation range of 600 to 800 mm (Bai et al. 2013).

## 2.2 Data source

In this study, we selected 19 meteorological stations in the Zoige Wetland and its surrounding areas based on the continuity requirement of meteorological data. Daily meteorological data from 1961 to 2016 were collected from the China Meteorological Data Service Center (CDMC) (<http://cdc.cma.gov.cn/home.do>) (Table 1), which is responsible for data quality control and management of the Climate Data Center. However, two of the stations have data missing and the missing time is part of the month of 1967 and 1968. The data of the missing stations was interpolated based on the linear regression analysis method, and the results were examined by a series of strict quality control measures and the time consistency test to meet the requirements of homogeneity and stationarity. The data included precipitation ( $P$ , mm), maximum air temperature ( $T_{\max}$ , °C), minimum air temperature ( $T_{\min}$ , °C), mean air temperature ( $T_{\text{mean}}$ , °C), relative humidity ( $RH$ , %), wind speed at 10-m height ( $WS$ , m/s), sunshine duration ( $SD$ , h), and atmospheric pressure ( $p$ , kPa). Meteorological seasons were considered as winter (December, January, and February), spring (March, April, and May), summer (June, July, and August), and autumn (September, October, and November) according to China's meteorological standard.

## 2.3 Methods

### 2.3.1 Calculation of potential evapotranspiration

The principle of SPEI is using the degree of distinction between precipitation and potential evapotranspiration (PET) which deviates from the average status to represent the regional drought conditions (Vicente-Serrano et al. 2010). PET could

be estimated by either the Thornthwaite method (Thornthwaite, 1948), Hargreaves method (Hargreaves and Samani 1985), or Penman–Monteith (PM) method (Allen et al. 1998). The equations used to compute PET can have manifest effects on SPEI in certain regions of the world (Begueria et al. 2013). Among these calculation means, the physical-based PM method is one of the most widely accepted and used ways to calculate PET, which has been resorted by the Food and Agriculture Organization of the United Nations (FAO), the International Commission on Irrigation and Drainage (ICID), and the American Society of Civil Engineers (ASCE) as the standard procedure for calculating PET (Vicente-Serrano et al. 2010). The PET computed by PM method takes not only air temperature but also wind speed, relative humidity, and sunshine duration into consideration, which thus fits with the measured PET values in arid or wet regions (Wang et al. 2015). Therefore, PET was calculated based on the United Nations Food and Agriculture Organization PM method (Allen et al. 1998):

$$PET = \frac{0.408\Delta(R_n - G) + \gamma \frac{900}{T + 273} U_2 (e_s - e_a)}{\Delta + \gamma(1 + 0.34U_2)} \quad (1)$$

where PET is potential evapotranspiration (mm);  $\Delta$  is slope of the vapor pressure curve ( $\text{kPa } ^\circ\text{C}^{-1}$ );  $\gamma$  is the psychrometric constant ( $\text{kPa } ^\circ\text{C}^{-1}$ );  $U_2$  is wind speed at 2-m height (m/s);  $R_n$  is net radiation at the surface ( $\text{MJ/m}^2$ );  $G$  is soil heat flux density ( $\text{MJ/m}^2$ );  $T$  is mean daily air temperature (°C);  $e_s$  and  $e_a$  are saturation vapor pressure (kPa) and actual vapor pressure (kPa) respectively. Variables are calculated according to the FAO method, except for  $R_n$ , which should be calibrated (Fan et al., 2018, 2019). In this paper, the calibrated radiation coefficient by Yin et al. was used to calculate  $R_n$  (Yin et al. 2008):

$$R_n = 0.77 \times \left(0.2 + 0.79 \frac{n}{N}\right) R_{so-\sigma} \left[ \frac{T_{\max,k}^4 + T_{\min,k}^4}{2} \right] \quad (2)$$

$$(0.56 - 0.25\sqrt{e_a}) \left(0.1 + 0.9 \frac{n}{N}\right)$$

**Table 1** Geographical location and elevation of the 19 meteorological stations used in this study

Station	Latitude (°N)	Longitude (°E)	Elevation (m)	Station	Latitude (°N)	Longitude (°E)	Elevation (m)
Pingwu	32.42	104.52	877.4	Aba	32.90	101.70	3276.6
Jiuzhaigou	33.27	104.23	1406.8	Rangtang	32.27	100.98	3286.6
Maoxian	31.68	103.85	1591.6	Ruoergai	33.58	102.97	3441.1
Heishui	32.08	102.98	2400.1	Maqu	34.00	102.08	3473.2
Diebu	34.07	103.22	2401.4	Hongyuan	32.80	102.55	3492.7
Maerkang	31.90	102.23	2665.9	Henan	34.73	101.60	3501
Lintan	34.70	103.35	2811.6	Banma	32.93	100.75	3530
Songpan	32.65	103.57	2852.1	Jiuzhi	33.43	101.48	3630
Hezuo	35.00	102.90	2910.5	Guoluo	34.47	100.25	3720
Luqu	34.58	102.50	3106.7				



where  $\sigma$  is Stefan–Boltzmann constant ( $4.903 \times 10^{-9}$  MJ/K<sup>4</sup> m<sup>2</sup>);  $n$  is the actual sunshine hours (h);  $N$  is the maximum sunshine hours (h);  $R_{so}$  is the sunny day radiation (MJ/m<sup>2</sup>);  $T_{\max, k}$  and  $T_{\min, k}$  are the maximum air temperature (K) and the minimum air temperature (K), respectively.

Due to the lack of  $U_2$  data, this variable was estimated from wind speed at 10-m height by adopting the logarithmic vertical wind speed profile (Allen et al. 1998):

$$U_2 = U_z \frac{4.87}{\ln(67.8z - 5.42)} \quad (3)$$

where  $z$  is the height of measurement above ground surface (m) and  $U_z$  is the measured wind speed at  $Z$  m above ground surface (m/s).

The detailed description used in estimating PET was given in Chapter 3 of FAO–56 (Allen et al. 1998). The monthly values of PET were calculated using daily PET data.

### 2.3.2 Calculation of SPEI

The worldwide used Standardized Precipitation Evapotranspiration Index (SPEI) was adopted in this study to monitor and quantify variations in drought conditions in the Zoige Wetland, Southwest China. The calculation of the SPEI in our study followed the method mentioned in the reference (Vicente-Serrano et al. 2010). Positive values of SPEI indicate the above average moisture conditions while negative values indicate the drier conditions (Li et al. 2015a, b). The nine types of dry/wet categories based on the SPEI values are listed in Table 2 (Li et al. 2015a, b; Li et al. 2014a, b; Olusola et al. 2017).

### 2.3.3 Statistical test for trend analysis

The Mann–Kendall (MK) analysis, a non-parameter method, was widely applied to make trend and mutation analysis of time series, UF is a time series statistical curve, and UB is an inverse time series statistical curve. The intersection of the two curves in the confidence interval is a

**Table 2** Categorization of dryness/wetness grade by SPEI

Categories	SPEI values
Extremely wet	2.00 and above
Very wet	1.50 to 1.99
Moderately wet	1.00 to 1.49
Slight wet	0.50 to 0.99
Near normal	−0.49 to 0.49
Slight dry	−0.50 to −0.99
Moderately dry	−1.00 to −1.49
Severely dry	−1.50 to −1.99
Extremely dry	−2.00 and less

changing point (Yang et al. 2016). The advantage of the MK analysis is that the sample series does not need a certain distribution, nor be interfered by minor outliers, so it fits for all kinds of variables and sequence variables (Zhang et al. 2017). In our study, the MK analysis was used to detect abrupt mutation of SPEI and determine trends of climatic factors and their significance on different time scales.

Furthermore, the Theil–Sen slope estimator was used to determine the extent of SPEI. This technique is generally applied to detect the slope of the trend line in a hydro-meteorological time series dataset (Hosking 1990; Yue et al. 2002; Fan et al., 2016). The Theil–Sen slope estimator was calculated as follows:

$$\beta = \text{median} \left( \frac{x_j - x_i}{j - i} \right) \quad (4)$$

where  $\beta$  is the Theil–Sen slope estimator (Thiel, 1950; Sen, 1968),  $x_j$  and  $x_i$  are the observed value corresponding to time  $j$  and  $i$ , respectively. When  $\beta$  is negative, it demonstrates a downward trend, i.e., the variable decreases with the increase of time and vice versa.

### 2.3.4 Periodical analysis

Wavelet transform has been widely used in the fields of climatic and hydrological changes (Zhao et al. 2012). Especially, the continuous wavelet transform (CWT) introduced by Torrence and Compo (Torrence and Compo 1998) has been widely applied to research the periodicity of drought condition variations (Wang et al. 2017). In our study, the Morlet wavelet analysis was used to calculate the periodicity of SPEI variations, because the Morlet wavelet function shows a good balance between the time and frequency localizations and is preferred for application (Wang et al. 2017). The effect of introducing a cone of influence (COI) to ignore the edge effect of the wavelet is not fully localized in time. In this study, COI is the region of  $e^{-2}$  where the wavelet power caused by the discontinuities at the edge dropped to the edge value followed by Wang et al. (2017). The 95% confidence interval is the range of confidence of a given value (Torrence and Compo 1998).

### 2.3.5 Partial correlation coefficients

The variations of drought conditions are mainly attributed to the changes and comprehensive effects of various meteorological elements. In order to understand the causes of SPEI changing characteristics, the partial correlation analysis was adopted in our study (Zhao et al. 2013). Partial correlation analysis is one kind of numerous correlation analysis methods. In this method, the partial correlation coefficient (PC) was

used to characterize the linear correlation between two variables under the condition that other variables are controlled, and the closer the absolute value of partial correlation coefficient to 1, the higher the correlation between these two variables (Tan et al. 2017).

### 2.3.6 Spatial interpolation

In order to analyze the spatial patterns of the magnitudes and trends of SPEI, the Inverse Distance Weighting algorithm (IDW) was used, which is widely applied all over the world to map the spatial extent of climatic and hydrological point data for giving the lowest mean error (Feng et al. 2017; Qi et al. 2017; Ma et al. 2017). The method is a deterministic interpolation assuming that the sample values closer to the prediction location are more representative than sample values farther away (Ashraf and Routray 2015). Thus, the closest value to the prediction location receives the maximum weight and the weight is decreased as a function of distance (Palizdan et al. 2017). In this study, the power parameter  $\alpha$ , which controls the significance of the predicted location values, was defined as 2 by following Palizdan et al. (2017). All spatial interpolations were conducted making use of the ArcGIS 10.1 software.

## 3 Results

### 3.1 The interannual variability of SPEI value on an annual and seasonal scale

The SPEI value as a meteorological drought index corresponds with dry/wet conditions, and a lower SPEI value signifies a more severe drought condition (Tong et al. 2018). The 12-month and 3-month SPEI, which were computed from the regional series of PET and precipitation across the Zoige Wetland for the period 1961–2016, reflected annual and seasonal drought conditions, respectively (Fig. 2). Figure 2 a (left) showed the interannual variability of the annual SPEI value of the Zoige Wetland. It could be observed from Fig. 2a (left) that the annual SPEI value of the entire wetland had shown a decreasing trend over the past 56 years at a tendency rate of  $-0.142/(10 \text{ years})$ . Nearly half of the annual SPEI values were negative with some years less than  $-1.0$ , and the value of the year 2002 reached to the minimum value of  $-2.42$ , which means the most severe drought of the studied period. The accumulated departure can judge the changing trend and phase of time series. From the accumulated departure curve on an annual scale in Fig. 2a (left), the annual SPEI accumulated departure increased from 1961 to 1968 and decreased sharply from 1969 to 1974. Then the annual SPEI accumulated departure increased slowly and peaked at about 7.19 in 1993 and dropped until 2016, showing a manifest

drying trend in recent years. The curve showed that the drought intensity varied over time. It was gradually weakened in the 1960s, gradually strengthened at the beginning of 1970s, then continuously decreased from the early 1970s to early 1990s and finally strengthened continuously from the early 1990s to 2016.

Figure 2 b–e (left) demonstrate the interannual variability of SPEI value in the four seasons. From Fig. 2b (left), all of the spring SPEI values were negative, and nearly one-third of the values were less than  $-1.5$  with the year 1984 being below  $-2$ . However, spring experienced a fluctuant increasing change at a rate of  $0.014/(10 \text{ years})$ , which means the Zoige Wetland varied tardily from dryness to wetness in spring. The spring accumulated SPEI departure curve in Fig. 2b (left) presented a “decreasing–increasing–slightly decreasing” trend, demonstrating the spring drought aggravated from 1961 to late 1980s, then lessened until the beginning of the 2000s, followed by slight exacerbation up to 2016. Figure 2 c–e (left) presented a similar drying trend of SPEI in summer, autumn, and winter, and the SPEI in the three seasons followed the order: autumn ( $-0.085/(10 \text{ years})$ ) > summer ( $-0.027/(10 \text{ years})$ ) > winter ( $-0.004/(10 \text{ years})$ ). Most years of summer and autumn were dominated by humid climate; nevertheless, drought was the main climate type in winter. In Fig. 2c (left), the summer accumulated SPEI departure increased until 1967 and decreased until 1971 briefly, then showed an ascending trend demonstrating humidity from 1972 to 1999, after that, dropped sharply until 2009, and slowly increased in recent 6 years, showing the most fluctuant variations of drought among annual and seasonal scales. In Fig. 2d (left), the autumn accumulated SPEI departure experienced an undulant variation with the wetland predominated by moist climate on autumn scale. Though summer and autumn mainly were humid in recent 56 years, the tendency rate and accumulated departure both indicated a trend towards drought forward, especially in autumn, with the Z value of  $-2.38$  (passed 0.05 confidence level). From Fig. 2e (left), the winter accumulated SPEI departure had a similar alteration to spring. The “decreasing–increasing–slightly decreasing” trend of accumulated departure indicated that the wetland swerved to drought since 2004 and the drought might be more severe in winter.

Figure 2 (right) shows the mutation of SPEI on different time scales by MK test. From Fig. 2d (right), the two curves intersected in 1983 at a significance level of 0.05 (correspondingly the threshold value for the UF and UB curves is  $\pm 1.96$ ), which was an evident abrupt mutation point of SPEI on an autumn scale. After 1983, the UF curve decreased significantly and crossed the threshold value after 1996; thus, the autumn SPEI exhibited an obvious change from humidity towards drought since 1983. In Fig. 2 a–c (right) and e (right), there were many other intersections between the two curves of UF and UB in the critical region, so it was not certain whether these intersections were mutation points.

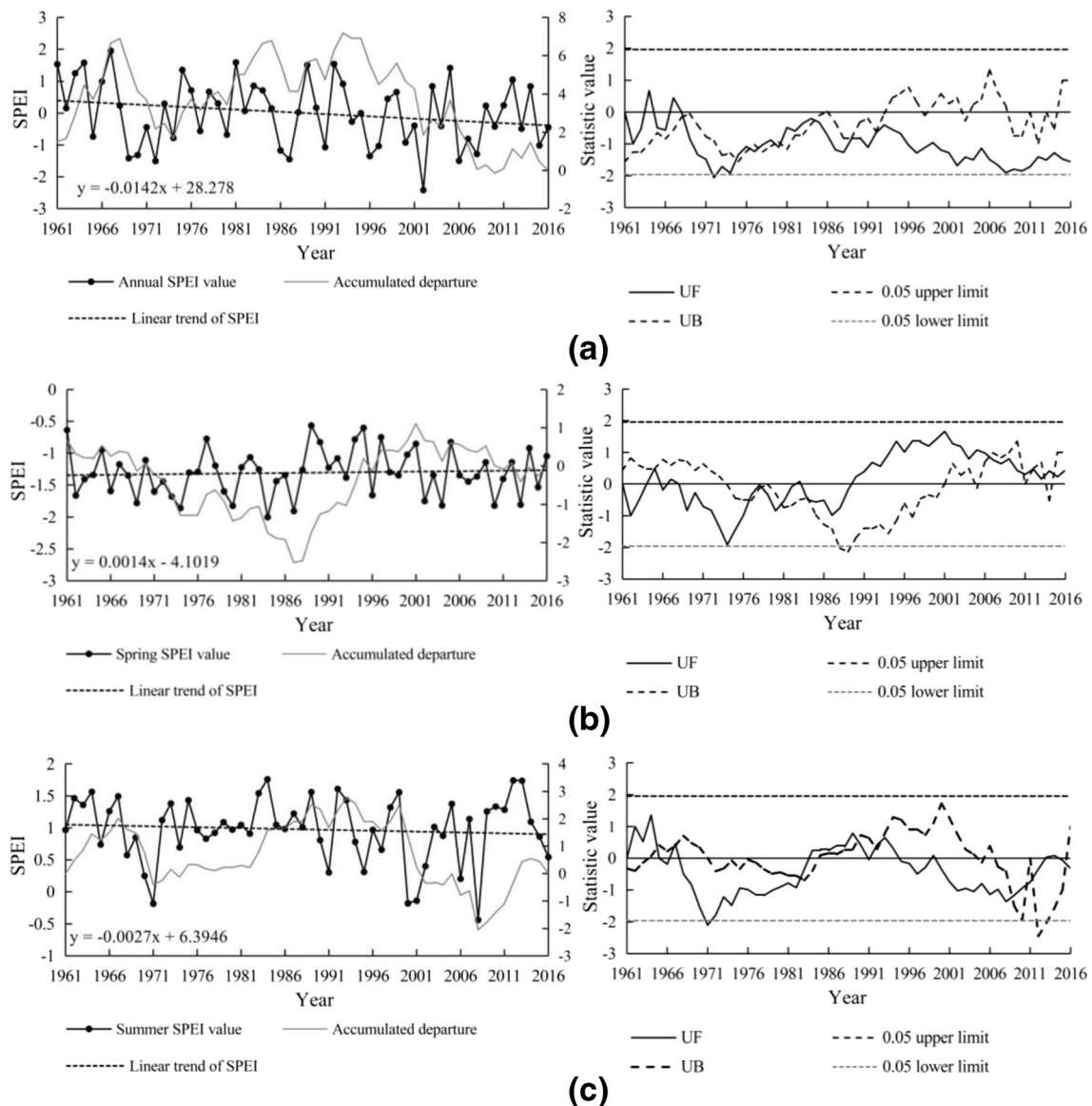


**Fig. 2** The interannual variability of and mutation test of annual (a), spring (b), summer (c), autumn (d), and winter (e) SPEI value (left) and MK test (right)

### 3.2 Periodic variations of SPEI value on annual and seasonal scales

Figure 3 shows the power spectrum and the time-average power spectrum of annual and seasonal SPEI in Zoige Wetland after the Morlet wavelet transform. The high wavelet power is orange, and low powers are blue and white. The thick black contour outline on the left side represents the 95% confidence level against red noise, while the edge effect may cause the image distortion cone (COI) to appear as a brighter bell shadow. The dotted line in the right part represents the 95% confidence level for the red noise null hypothesis, and the corresponding period is significant if the peak of the full line exceeds the dashed line in the power graph (Wang et al. 2017). Figure 3 a shows that the periods of 2.4, 3.2, and

6.0 years of the annual SPEI series all passed the 95% confidence level test from 1961 to 2016. The intensity of these cycles changed over time. Interannual oscillations of 2–5 years were noticed in the period of 1961–1972 within the 95% confidence level. Significant interannual oscillations at 2–3-year scale were observed from 1970 to 1983. In addition, interannual oscillations at 2–8-year scales were observed during the period of 1984–2016, with significant difference during 1984–2008 at the 95% confidence level.

In Fig. 3b, the periods of 3.0, 6.0 years of the spring SPEI series are significantly above the 95% confidence level, and interannual oscillations of 2–4-years as well as 2–8-years in the period of 1961–1975 and 1972–2008 are within the 95% confidence level. In Fig. 3c, the periods of 3.0 and 6.0 years of the summer SPEI series existed significantly above the 95%

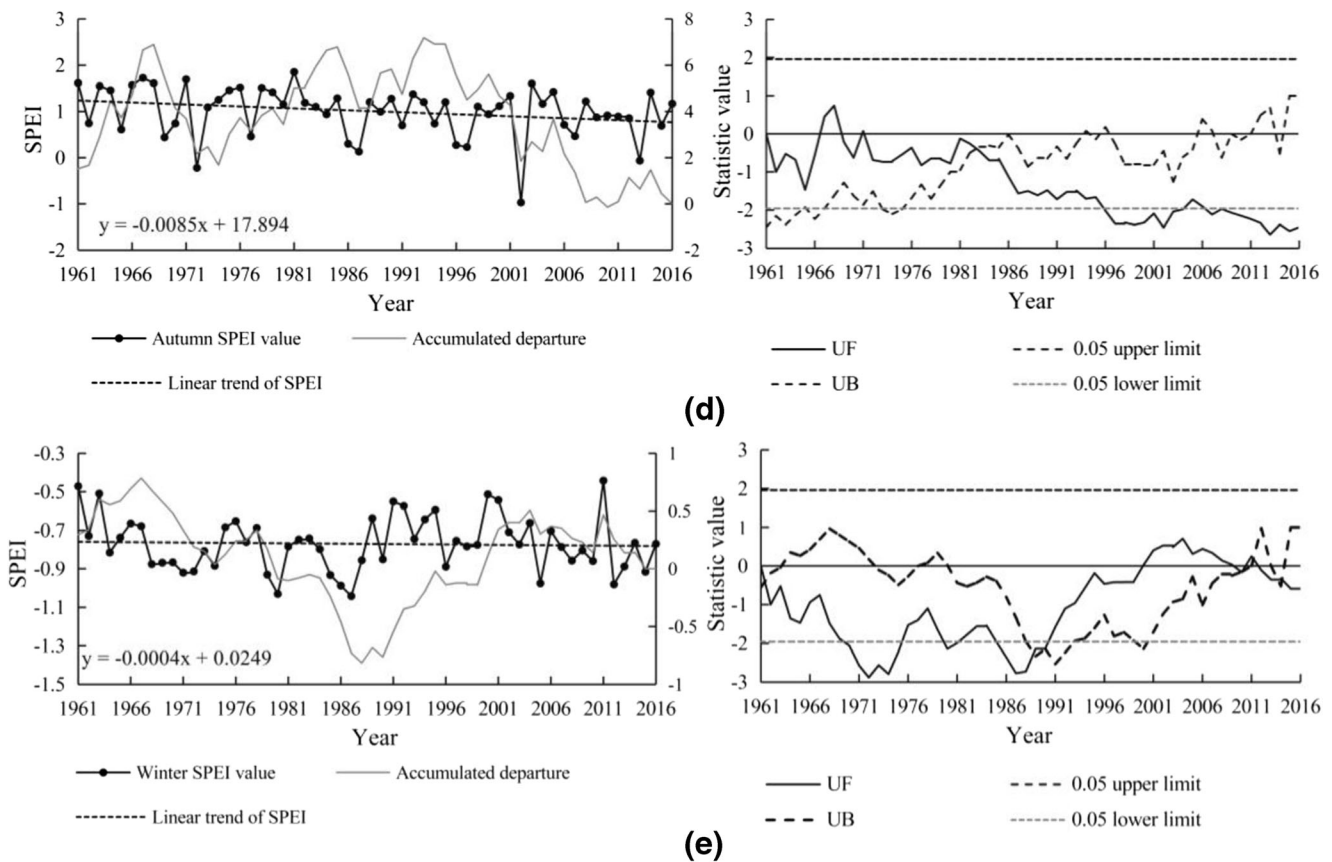


Fig. 2 (continued)

confidence level, besides, interannual oscillations of 2–4 years as well as 2–8 years were observed in the period of 1965–1975 and 1972–2005 at the 95% confidence level, respectively. In Fig. 3d, the periods of 2.8, 3.0, and 4.8 years of the autumn SPEI series exist at the 95% confidence level, and interannual oscillations of 2–8 years were noticed in the period of 1961–2010 at the 95% confidence level. In Fig. 3e, only the periods of 3.0 year of the winter SPEI series exist at the 95% confidence level, besides, interannual oscillations of 2–4 years were observed in the period of 1961–1966, 1975–1982, and 1988–2016 significantly above the 95% confidence level. However, interannual oscillations of 6–9 years observed in the period of 1977–2000 are significantly below the 95% confidence level.

### 3.3 Spatial distribution of SPEI and its trend

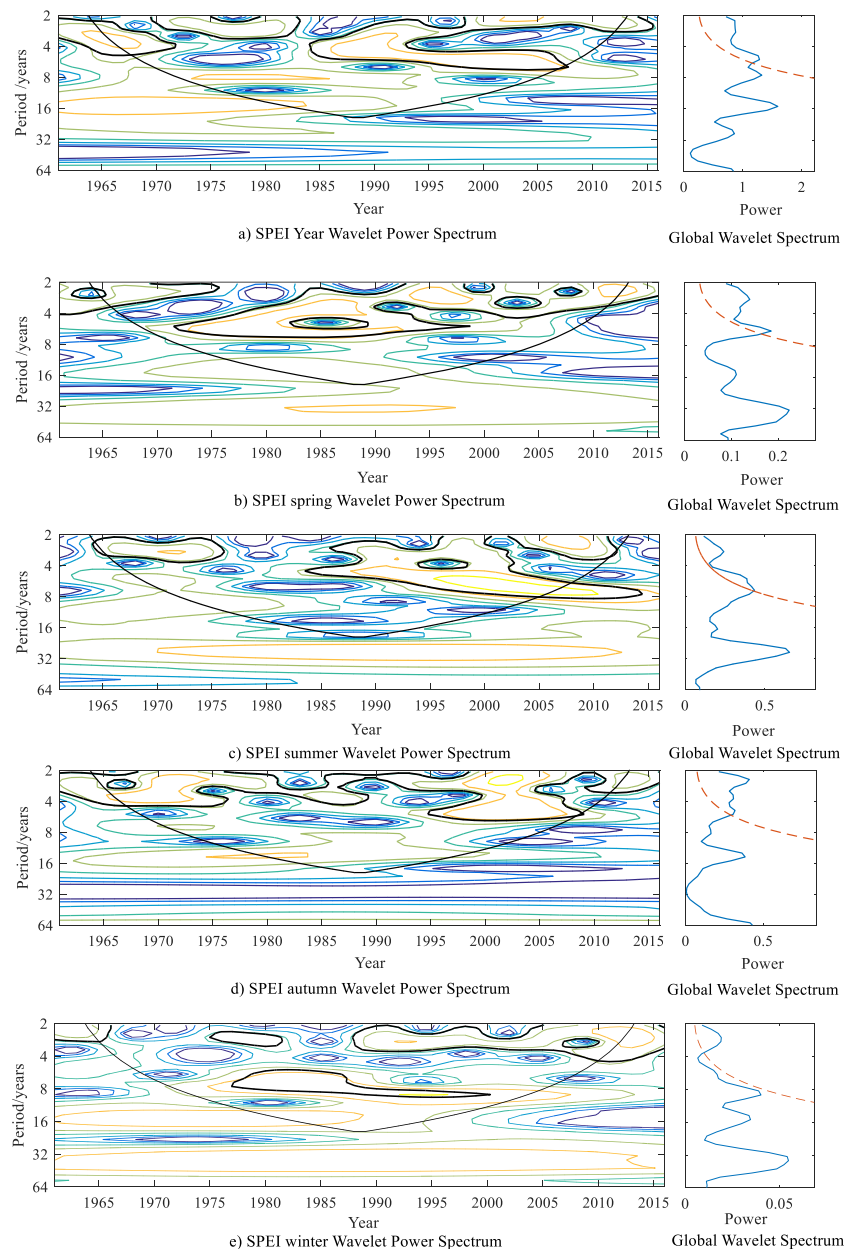
In Fig. 4 b–e (left), the average SPEI of spring, summer, autumn, and winter is  $-1.306$ ,  $0.977$ ,  $1.005$ , and  $-0.770$ , respectively. In Fig. 4b (left), the overall spatial distribution of SPEI in spring presents a decreasing trend from the southeast to the northwest. The high SPEI was primarily concentrated in Songpan County, southeast of the wetland, with a maximum value of  $0.019$ , and the overall wetland presented drought of different degrees on spring scale. Figure 4 c (left) shows that

the overall wetland presented humid with an increasing trend from the north and southeast to the south and west of the wetland on summer scale. In Fig. 4d (left), it presented that the overall wetland was humid on the autumn scale. The high SPEI was mainly concentrated in Ruergai County, north of the Zoige wetland, with a maximum value of  $1.044$ , while the low SPEI was mainly distributed in Songpan County, southeast of the wetland, with a minimum value of  $0.700$ . From Fig. 4e (left), the areas with the value of SPEI below  $-0.5$  accounted for 84.77% of the total area of the Zoige Wetland, indicating that most areas showed drought in winter. However, the value of SPEI presented a tendency of decreasing gradually from the north to the south of the wetland.

In Fig. 4 b–e (right), the spatial distribution of the climate tendency rate of SPEI ( $\beta$ ) had obvious differences in different seasons. In spring, the overall drought was alleviated due to positive tendency with the maximum of  $0.086/(10 \text{ years})$ , except for individual sites in Ruergai County with a sharp decreasing rate of  $-0.242/(10 \text{ years})$ . The spatial distribution of the climate tendency rate of SPEI of summer was similar to spring, but the wetland had a drying trend in most areas except the south of the wetland. In autumn, all the Theil–Sen slope estimator values ( $\beta$ ) were below 0, which meant the trend towards drought in the whole wetland, and the value of  $\beta$  had a decreasing tendency from southern to northern wetland.



**Fig. 3** Morlet wavelet spectrum analysis of annual (a), spring (b), summer (c), autumn (d), and winter (e) SPEI



In winter, the value of SPEI only in Jiuzhi County and part of southern wetland had an increasing trend, and the majority of areas of the wetland had a manifest drying trend with a minimum value of  $-0.037/(10 \text{ years})$ . Generally, the tendency of drought increased significantly overall in autumn, followed by summer and winter, but mainly mitigated in spring.

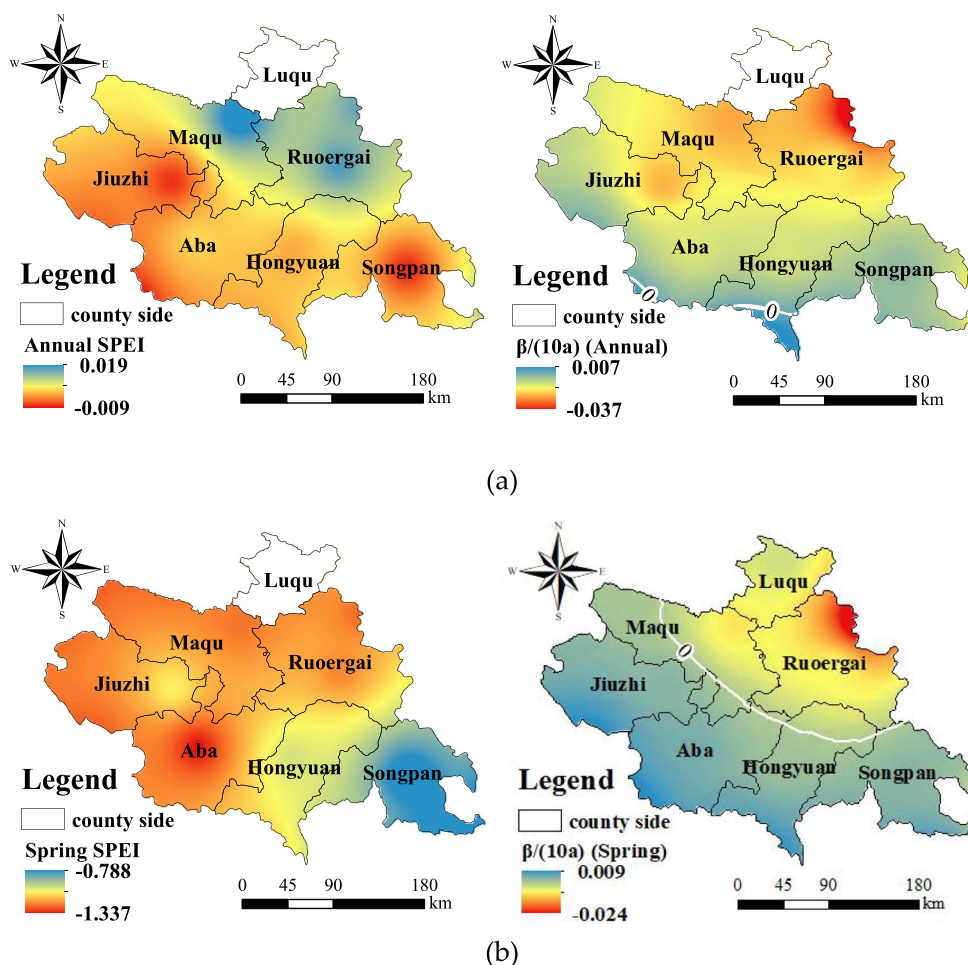
### 3.4 Attribution analysis of SPEI

Precipitation and potential evapotranspiration (PET) are the main parameters for calculating SPEI. In our study, the PET was computed by the Penman–Monteith method, which took not only air temperature but also wind speed, relative humidity, and sunshine duration into consideration (Wang et al.

2015). Therefore, precipitation, mean temperature, relative humidity, wind speed at 2-m height, and sunshine duration were regarded as the main factors affecting SPEI. The MK trend analysis of each factor and the partial correlation analysis of each factor to SPEI were carried out in this study, and the result is illustrated in Table 3.

In Table 3, positive  $Z$  values demonstrate an increasing tendency while negative values represent a decreasing trend, and trends in climatic factors are considered significant if the estimated  $Z$  value falls below a critical value ( $\alpha < 0.05$ ) at 0.05 confidence level. The Zoige Wetland experienced a significant increase in mean temperature on both annual and seasonal scales during 1961–2016, with the mean temperature on an annual scale being the highest ( $Z = 6.55$ ), and the lowest in

**Fig. 4** The spatial variability of annual (a), spring (b), summer (c), autumn (d), and winter (e) SPEI value (left) and the climate tendency rates of SPEI ( $\beta$ ) (right)



spring ( $Z = 3.77$ ). Relative humidity showed a decreasing trend on all time scales, among which only winter failed at 0.05 confidence level, and summer indicated the most significant decreasing trend ( $Z = -4.45$ ). Wind speed at 2-m height indicated a significant decreasing trend on both annual and seasonal scales and the sharpest decrease was in spring ( $Z = -3.31$ ). Sunshine duration arose in autumn and declined on the rest time scales, but the trends were not significant. Precipitation only replied an increasing trend significantly in spring and winter, while decreased on other time scales with the failure of 0.05 confidence test.

In Table 3, the partial correlation coefficients of different climatic factors to SPEI were quite different, and the influence of each factor on SPEI varied on different time scales. During 1961–2016, the partial correlations of precipitation, wind speed at 2-m height, and sunshine duration to SPEI were the highest, which also passed the 0.05 confidence test and mainly affected annual SPEI, followed by mean temperature and relative humidity. In spring, SPEI had a higher correlation with wind speed at 2-m height, relative humidity, and sunshine duration at the significance level of 0.05. In summer, precipitation mainly affected SPEI at the significance level of 0.05 as the highest factor

among partial correlations. In autumn, sunshine duration, precipitation, and relative humidity, as the highest factors among partial correlations, mainly affected SPEI at the significance level of 0.05. In winter, SPEI had the highest correlation with wind speed at 2-m height at the significance level of 0.05. Specifically, SPEI has a positive correlation with precipitation and relative humidity on all time scales. The highest correlation with precipitation and relative humidity was on an annual scale ( $PC = 0.985$ ) and in spring ( $PC = 0.356$ ) respectively, indicating that the increase in precipitation and relative humidity was conducive to the increase of SPEI on corresponding time scales. Negatively correlated with SPEI on all time scales, the variations of mean temperature led to inverted variations of SPEI. SPEI was negatively correlated with wind speed on annual, spring, and winter scales but positively correlated on others, while negatively correlated with sunshine duration on annual and winter scale but positively correlated on others.

Overall, the drought condition variations of the Zoige Wetland resulted from the comprehensive meteorological factors, where precipitation, relative humidity, wind speed at 2-m height, and sunshine duration played different roles of

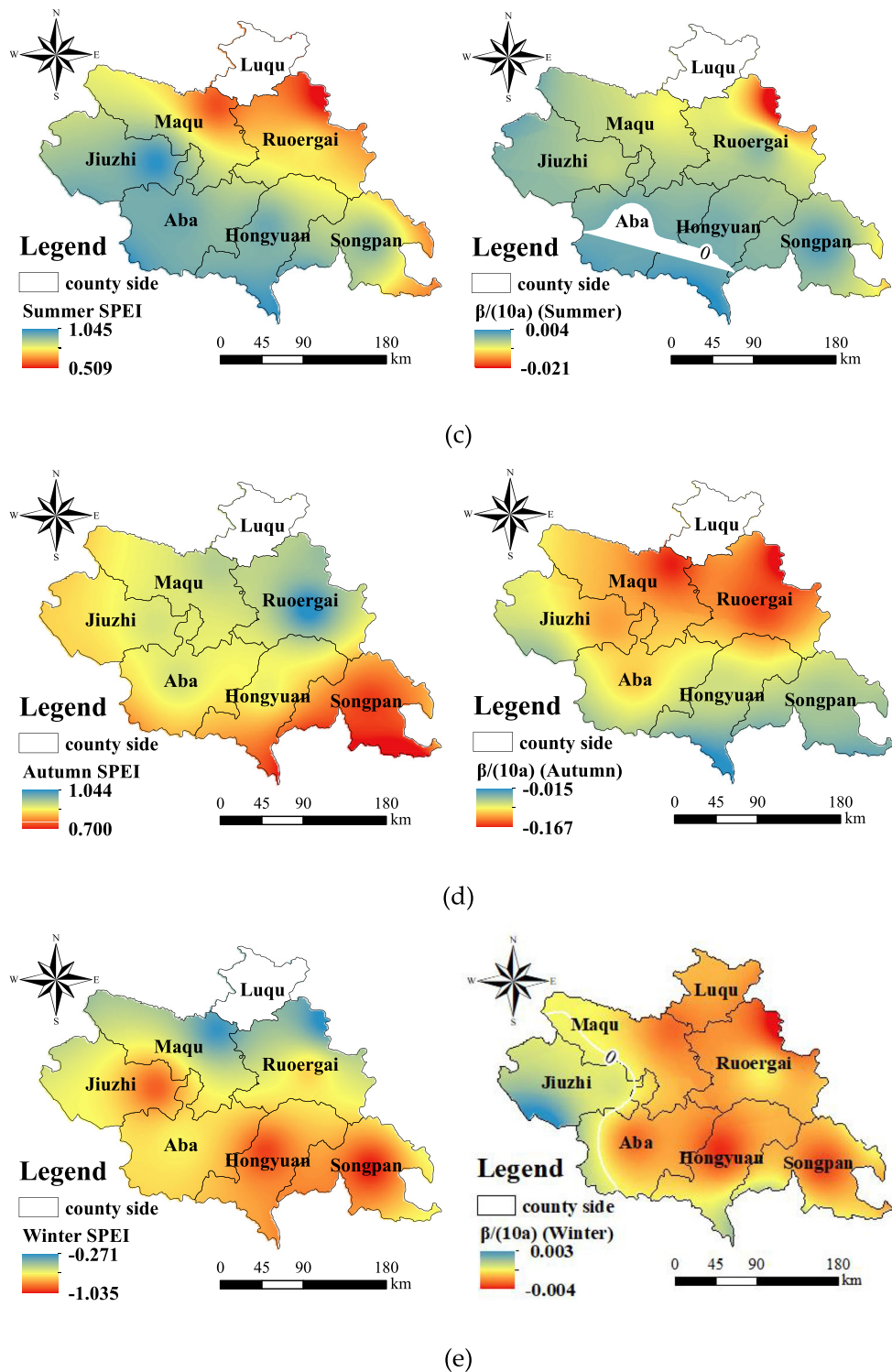


Fig. 4 (continued)

importance on various time scales while mean temperature was the weakest climatic component through. The decrease of annual SPEI was primarily due to the decrease of precipitation, followed by mean temperature increase and relative humidity decrease, which offset the reversed impact of wind speed decrease and sunshine duration decrease. In spring and

winter, most of the years were also dominated by arid climate, while spring was experiencing a fluctuant humidity tendency with the result of the significant increase in precipitation and significant decrease in wind speed, while winter was experiencing drought intensity for significant increase in mean temperature. In summer and autumn, most of the years were

**Table 3** The trend analysis of each factor (*Z*) by MK test and partial correlation coefficients (PC) between climate factors and SPEI

Time scale	Year	Statistic index	Precipitation	Mean temp.	Relative humidity	Wind speed at 2-m height	Sunshine duration
Whole year	1961–2016	<i>PC</i>	0.985*	− 0.203	0.195	− 0.719*	− 0.676*
		<i>Z</i>	− 1.62	6.55*	− 3.94*	− 2.64*	− 0.09
Spring	1961–2016	<i>PC</i>	0.214	− 0.018	0.356*	− 0.401*	0.293*
		<i>Z</i>	2.59*	3.77*	− 3.36*	− 3.31*	− 0.01
Summer	1961–2016	<i>PC</i>	0.381*	− 0.240	0.229	0.021	0.017
		<i>Z</i>	− 1.20	5.30*	− 4.45*	− 2.23*	− 0.18
Autumn	1961–2016	<i>PC</i>	0.385*	− 0.024	0.313*	0.021	0.441*
		<i>Z</i>	− 1.31	4.82*	− 3.74*	− 1.76	0.33
Winter	1961–2016	<i>PC</i>	0.055	− 0.090	0.031	− 0.338*	− 0.036
		<i>Z</i>	2.15*	4.72*	− 1.13	− 1.62	− 0.49

“\*” means passing the 0.05 confidence test for trend analysis (*Z*), while “\*\*” means significance level  $P < 0.05$  for partial correlation coefficients (*PC*)

dominated by humid climate while they were both experiencing the trend towards aridity for obvious reduction of precipitation and relative humidity and rising of mean temperature.

## 4 Discussion

Based on the Penman–Monteith method, this study calculated the SPEI to characterize the drought variations during 1961–2016 on annual and seasonal scales in the Zoige Wetland, the eastern fringe of the Tibetan plateau. Results indicated that the Zoige Wetland tended to be warmer and obviously drier. However, Mao et al. (2008) reported that most areas of the Tibetan Plateau had a warming and wetting trend in recent years. Yang et al. (2009) found that Ali and Naqu counties, located in the northwest of Tibet, were developing the tendency of warming–drying and warming–wetting respectively. Wang et al. (2013) assessed the changes of potential evapotranspiration and surface moisture in the northeast of Tibetan Plateau and found that the grassland of Hezuo County had a warming and drying trend, which was different from the tendency of humid climate development in the main plateau, and also different from the trend of warming and humidification in the source area of the Yellow River since the twenty-first century. From these results above, we concluded that different geographical locations of the Tibetan plateau presented different drought/wetness condition variations under the same climatic background. Thus, more detailed researches on climatic variations of different parts of the Tibetan Plateau are needed in the future. The Zoige Wetland tended to be warmer and drier, which will exacerbate surface water deficits, lead to an increase in the area affected by drought and aggravation of pest diseases, and intensify the degradation and desertification of wetlands. Therefore, effective measures must be taken to deal with the seriously increasing aridity of the Zoige Wetland.

Generally, a 2–8-year significant period was discovered on both annual and seasonal scales, which is the same as China’s experiencing a significant 2–8-year period (Wang and Wei 2016). This may be related to the ENSO phenomenon, which is known to impact general atmospheric circulation worldwide, causing climatic factors like precipitation and temperature to fluctuate over 2–8-year periods (Dai, 2012; Liu et al. 2016a, b). Thus, the temporal periodicity of drought variations may be affected by the ENSO by affecting climatic factor changes. In addition, the power spectrum showed that SPEI on an annual scale had undergone significant cycle adjustments from around the end of the 1980s to the end of the 1990s, which may lead to manifest transformations of hydro-thermal conditions of the wetland. It is worth noting that obvious change from humidity towards drought of autumn SPEI was also in this interval. Among different time scales, SPEI showed the shortest significant period (less than 4 years) in winter. Furthermore, due to overall drought in winter, measures must be taken to improve the capacity of the wetland to cope with the winter drought.

Precipitation and potential evapotranspiration are the main parameters for calculating SPEI. Sun et al. (2016) found that the contribution of potential evapotranspiration to the drought/wetness changes in the southwestern region of China is comparable with that of precipitation, and pointed out that the effect of potential evapotranspiration on local dry–wet changes and drought is worthy of attention. Therefore, the variation of drought conditions is in general strongly related to meteorological factors, such as precipitation and temperature. The results of the partial correlations in this study confirmed that the precipitation is the most important factor affecting the variations of drought conditions. The results are basically consistent with the existing research conclusions. For example, Su et al. (2014) found that precipitation is the decisive factor for the drought and wetness



conditions of China's southwestern region. Meanwhile, meteorological factors such as relative humidity also have a great impact by affecting the potential evapotranspiration. Temperature plays an important role in drought changes as well (Liu and Jiang 2015). Chen and Sun (2017) found that the sustained and significant increase in China's drought in the past 20 years was mainly related to the sharp increase in temperature and the absence of great changes in precipitation. We found that the increase in temperature does promote the warming and drying trend of the wetland to a certain extent. However, due to the unique meteorological and hydrological conditions of the Zoige Wetland, changes in precipitation (especially in spring and winter) played a significant role in the wetland drought variations, which is a point that should be noted. From the spatial analysis perspective, the changes in wetland landscape patterns in Zoige County (Bai et al., 2013) showed that there were a large number of marsh wetlands in Ruorgai County in 1966, but most marsh wetlands disappeared after 1986, especially in the northeast part of the county. This matches the tendency pattern of SPEI ( $\beta$ ) in Fig. 4b–e (right) that the northeastern region of Ruorgai County showed the sharpest decreasing rate of SPEI, indicating the most severe trend towards drought. Bai et al. (2013) also found that both the annual precipitation and the surface runoff outflow showed a decreasing trend from 1966 to 2000, indicating that the annual precipitation and surface runoff outflow began to decrease after wetland degradation. Meanwhile, the decreasing annual precipitation and surface runoff outflow might further promote wetland degradation, which is like a vicious circle.

We only considered climatic elements in the study, but the drought/wetness variations in the Zoige wetland are not only related to climatic elements but also influenced by human activities and underlying surface elements such as recharge of ice and snow and runoff changes (Wang and Wei 2016). The rapid development of the economy has led to the continuous increasing demand of industrial and agricultural production and people's need for living water, resulting in over-exploitation of water resources in the area, leading to factors such as river cutoff, reduced vegetation coverage, declining groundwater level, and deterioration of water ecological environment, which contributed to regional drought development (Zhu and Chang 2017). What's more, the continuous growth of population in Zoige will lead to overgrazing and augment the pressure on wetland drainage and grassland degradation (You et al. 2017). As early as 1992, Zoige County carried out a desertification control experiment, but most relative studies have shown that the process of desertification was still expanding, only on certain periods or in certain regions, the desertification had abated. Thus, it is necessary to strengthen the quantitative study the effect of human activities and underlying surface elements on drought conditions in Zoige Wetland in the future.

## 5 Conclusions

In this study, drought condition variations during 1961–2016 were evaluated using SPEI based on the Penman–Monteith method on both annual and seasonal scales in the Zoige wetland. According to the analysis of spatial-temporal patterns of SPEI in the wetland, we found the following:

1. The analysis of interannual variability of SPEI on both annual and seasonal scales indicated that the annual SPEI had a decreasing trend over the past 56 years with a rate of  $-0.142/(10 \text{ years})$  in the Zoige Wetland. This indicates a tendency of drought in winter and spring. The summer and autumn seasons were relatively humid but showed a tendency to dryness. The severity of drought condition as from the driest to the wet is winter, spring, year, summer, and autumn. The changing pattern of SPEI at the significance level of 0.05 occurred in the autumn of 1983, indicating that the humidity gradually turned to dryness and there were no significant changes observed on other time scales.
2. The periods of 2.4, 3.2, and 6.0 years of the annual SPEI series existed in Zoige from 1961 to 2016, significantly above the 95% confidence level through the power spectrum and the time-average power spectrum. Spring, summer, autumn, and winter seasons had periodic oscillations of various time scales and a 2–8-year significant period was found both at the annual and seasonal scales.
3. The overall spatial distribution of SPEI on an annual scale presented that humid areas located in the northern part had a drying trend, while arid areas mainly concentrated in southern part were turning wet. However, the majority of the wetland had a drying trend on annual scale. The overall spatial distribution of SPEI on seasonal scale showed that the wetland presented dryness and the dry conditions showed a tendency of mitigation except the northeastern wetland in spring. In summer, the wetland mainly presented humidity but had a drying trend in most areas except the south of the wetland. In autumn, the overall wetland was humid on this scale and the trend towards drought was manifest in the whole wetland. In winter, most areas showed drought and only Jiuzhi County and part of southern wetland had an alleviating trend of drought.
4. Precipitation, relative humidity, wind speed at 2-m height, and sunshine duration have different roles, while mean temperature was the weakest climatic influencing factor. The decrease of annual SPEI was primarily due to the decrease of precipitation, the increase of the mean temperature, and the decrease of the relative humidity that offset the reversed impact of wind speed decrease and sunshine duration decrease. In spring, the fluctuant humidity tendency was the result of the significant increase

in precipitation and significant decrease in wind speed, while the trend towards aridity in summer and autumn was due to obvious reduction of precipitation and relative humidity and rising of mean temperature, and winter was experiencing drought intensity for significant increase in mean temperature.

**Acknowledgments** We would like to thank the National Climatic Centre of the China Meteorological Administration for providing the climate database used in this study.

**Funding information** This work was also financially supported by the National Key Research and Development Program of China (2016YFC0400206), National Natural Science Foundation of China (51779161), National Natural Science Foundation–Outstanding Youth Foundation (51922072), and National Key Technologies R&D Program of China (No. 2015BAD24B01).

## References

- Allen RG, Pereira LS, Raes D, Smith M (1998) Crop evapotranspiration guidelines for computing crop water requirements. FAO irrigation and drainage paper 56. Rome, Italy
- American Meteorological Society (AMS) (2004) Statement on meteorological drought. *B Am Meteorol Soc* 85:771–773
- Ashraf M, Routray JK (2015) Spatio-temporal characteristics of precipitation and drought in Balochistan Province, Pakistan. *Nat Hazards* 77:229–254
- Bai J, Lu Q, Zhao Q, Wang J, Ouyang H (2013) Effects of alpine wetland landscapes on regional climate on the Zoige Plateau of China. *Adv Meteorol* 2013:1–7
- Beguiería S, Vicente-Serrano SM, Reig F, Latorre B (2013) Standardized precipitation evapotranspiration index (SPEI) revisited: parameter fitting, evapotranspiration models, tools, datasets and drought monitoring. *Int J Climatol* 34:3001–3023
- Burke EJ, Brown SJ, Christidis N (2006) Modeling the recent evolution of global drought and projections for the twenty-first century with the Hadley Centre climate model. *J Hydrometeorol* 7:1113–1125
- Chen H, Sun J (2015) Changes in drought characteristics over China using the standardized precipitation evapotranspiration index. *J Clim* 28:281–299
- Chen HP, Sun JQ (2017) Anthropogenic warming has caused hot droughts more frequently in China. *J Hydrol* 544:306–318
- Dai A (2012) Increasing drought under global warming in observations and models. *Nat Clim Chang* 3(1):52–58
- Dubrovsky M, Svoboda MD, Trnka M, Hayes MJ, Wilhite DA, Zalud Z, Hlavinka P (2009) Application of relative drought indices in assessing climate-change impacts on drought conditions in Czechia. *Theor Appl Climatol* 96:155–171
- Fan J, Wu L, Zhang F, Xiang Y, Zheng J (2016) Climate change effects on reference crop evapotranspiration across different climatic zones of China during 1956–2015. *J Hydrol* 542:923–937
- Fan J, Wang X, Wu L, Zhang F, Bai H, Lu X, Xiang Y (2018) New combined models for estimating daily global solar radiation based on sunshine duration in humid regions: a case study in South China. *Energy Convers Manag* 156:618–625
- Fan J, Wu L, Zhang F, et al. (2019) Empirical and machine learning models for predicting daily global solar radiation from sunshine duration: a review and case study in China. *Renewable and Sustainable Energy Reviews*, 100: 186–212
- Feng Y, Cui N, Zhao L, Gong D, Zhang K (2017) Spatiotemporal variation of reference evapotranspiration during 1954–2013 in Southwest China. *Quat Int* 441:129–139
- Hargreaves GH, Samani ZA (1985) Reference crop evapotranspiration from temperature. *Appl Eng Agric* 1:96–99
- Hosking JRM (1990) L-moments: analysis and estimation of distributions using linear combinations of order statistics. *J R Stat Soc B* 52:105–124
- IPCC (2013) Climate change 2013: the physical science basis [M/OL]. Cambridge University Press, Cambridge, in press
- Jiang S, Yang R, Cui N, Zhao L, Liang C (2018) Analysis of Drought Vulnerability Characteristics and Risk Assessment Based on Information Distribution and Diffusion in Southwest China. *Atmosphere* 9 (7):239
- Li X, He BB, Quan XW, Liao ZM, Bai XJ (2015a) Use of the standardized precipitation evapotranspiration index (SPEI) to characterize the drying trend in Southwest China from 1982–2012. *Remote Sens* 7:10917–10937
- Li BQ, Zhou W, Zhao YY, Ju Q, Yu ZB, Liang ZM, Acharya K (2015b) Using the SPEI to assess recent climate change in the Yarlung Zangbo River Basin, South Tibet. *Water* 7:5474–5486
- Li YZ, Feng AQ, Liu WB, Ma XY, Dong GT (2017) Variation of aridity index and the role of climate variables in the Southwest China. *Water* 9:743
- Li ZW, Wang ZY, Zhang CD, Han LJ, Zhao N (2014a) A study on the mechanism of wetland degradation in Ruergai swamp. *Adv Water Sci* 25:172–180
- Li B, Liang Z, Yu Z, Acharya K (2014b) Evaluation of drought and wetness episodes in a cold region (Northeast China) since 1898 with different drought indices. *Nat Hazards* 71:2063–2085
- Liu K, Jiang DB (2015) Analysis of dryness/wetness over China using standardized precipitation evapotranspiration index based on two evapotranspiration algorithms. *Chin J Atmos Sci* 39(1):23–36
- Liu X, Luo Y, Yang T, Liang K, Zhang M, Liu C (2015) Investigation of the probability of concurrent drought events between the water source and destination regions of China's water diversion project. *Geophys Res Lett* 42:8424–8431
- Liu Z, Menzel L, Dong C (2016a) Temporal dynamics and spatial patterns of drought and the relation to ENSO: a case study in Northwest China. *Int J Climatol* 8:2886–2898
- Liu ZP, Wang YQ, Shao MA, Jia XX, Li XL (2016b) Spatiotemporal analysis of multiscalar drought characteristics across the Loess Plateau of China. *J Hydrol* 534:281–299
- Lou WP, Sun SL, Sun K, Yang XZ, Li SP (2017) Summer drought index using SPEI based on 10-day temperature and precipitation data and its application in Zhejiang Province (Southeast China). *Stoch Environ Res Risk Assess* 31:2499–2512
- Ma N, Zhang Y, Szilagyi J, Guo Y, Zhai J, Gao H (2015) Evaluating the complementary relationship of evapotranspiration in the alpine steppe of the Tibetan Plateau. *Water Resour Res* 51:1069–1083
- Ma QY, Zhang JQ, Sun CY (2017) Changes of reference evapotranspiration and its relationship to dry/wet conditions based on the aridity index in the Songnen Grassland, Northeast China. *Water* 9:316
- Mao F, Tang SH, Sun H, Zhang JH (2008) A study of dynamic change of dry and wet climate regions in the Tibetan Plateau over the last 46 years. *Chinese J Atm Sci* 32:499–507
- McKee TB, Doesken NJ, Kleist J (1993) The relationship of drought frequency and duration to time scales. In: *Proceedings of the Eight Conference on Applied Climatology*. American Meteorological Society, Anaheim, pp 179–184
- Min SK, Zhang X, Zwiers FW, Hegerl GC (2011) Human contribution to more-intense precipitation extremes. *Nature* 470:378–381
- Olusola O, Ayantobo Li Y, Song SB (2017) Spatial comparability of drought characteristics and related return periods in mainland China over 1961–2013. *J Hydrol* 550:549–567

- Palizdan N, Falamarzi Y, Huang YF, Lee TS (2017) Precipitation trend analysis using discrete wavelet transform at the Langat River Basin, Selangor, Malaysia. *Stoch. Environ Res Risk Assess* 31:853–877
- Palmer WC (1965) Meteorological drought. Research paper No. 45. Office of climatology, U.S. Weather Bureau, Washington
- Qi P, Zhang GX, Xu YJ (2017) Spatiotemporal changes of reference evapotranspiration in the highest-latitude region of China. *Water* 9: 493
- Sen P (1968) Estimates of the regression coefficient based on Kendall's tau. *J Am Stat Assoc* 63:1379–1389
- Su XC, Wang L, Li QL et al (2014) Study of surface dry and wet conditions in Southwest China in recent 50 years. *J Nat Res (in Chinese)* 29(1):104–116
- Sun SL, Chen HS, Wang GJ et al (2016) Shift in potential evapotranspiration and its implications for dryness/wetness over Southwest China. *J Geophys Res* 121(16):9342–9355
- Tan J, Ding JL, Dong Y, Yang AX, Zhang Z (2017) Decadal variation of potential evapotranspiration in Ebinur Lake oasis of Xinjiang. *Transactions of the CSAE* 33:143–148
- Tong SQ, Lai Q, Zhang JQ (2018) Spatiotemporal drought variability on the Mongolian Plateau from 1980–2014 based on the SPEI-PM, intensity analysis and Hurst exponent. *Sci Total Environ* 615: 1557–1565
- Törnros T, Menzel L (2014) Addressing drought conditions under current and future climates in the Jordan River region. *Hydrol Earth Syst Sci* 18:305–318
- Thomthwaite CW (1948) An approach toward a rational classification of climate. *Geogr Rev* 38:55–89
- Torrence C, Compo GP (1998) A practical guide to wavelet analysis. *Bull Am Meteorol Soc* 79:61–78
- Vicente-Serrano SM, Beguería S, López-Moreno JI (2010) A multiscalar drought index sensitive to global warming: the standardized precipitation evapotranspiration index. *J Clim* 23:1696–1718
- Wang W, Zhu Y, Xu RG (2015) Drought severity change in China during 1961–2012 indicated by SPI and SPEI. *Nat Hazards* 75:2437–2451
- Wang ZL, Li J, Lai CG (2017) Does drought in China show a significant decreasing trend from 1961 to 2009? *Sci Total Environ* 579:314–324
- Wang JB, Wang ZG, Wang SP (2013) The variety characters of potential evapotranspiration and soil surface humidity index in Hezuo, Gansu During 1961–2010. *J AL Resour Environ* 27: 159–164
- Wang FF, Wei Y (2016) Variability of drought during winter wheat at growth in Shihezi reclamation area. *Res Soil Water Conserv* 23: 238–247
- Wilhite DA (2005) Drought and water crisis: science, technology, and management issues. In: Wilhite DA (ed) *Drought as hazard: understanding the natural and social context*. Boca Raton, Taylor and Francis Group, pp 5–10
- WMO (2006) Drought monitoring and early warning: concepts, progress and future challenges. World Meteorological Organization, Report WMO-No. 100692-63-11006-9, pp 24
- Woodward C, Shulmeister J, Larsen J (2014) The hydrological legacy of deforestation on global wetlands. *Science* 346:844–847
- Xu K, Yang D, Yang H, Li Z, Qin Y, Shen Y (2015) Spatio-temporal variation of drought in China during 1961–2012: a climatic perspective. *J Hydrol* 526:253–264
- Yang MJ, Yan DH, Yu YD, Yang ZY (2016) SPEI-based spatiotemporal analysis of drought in Haihe river basin from 1961 to 2010. *Adv Meteorol* 2016:1–10
- Yang Q, Li MX, Zheng ZY (2017) Regional applicability of seven meteorological drought indices in China. *Scientia Sinica(Terrae)* 03: 81–97
- Yang XH, Zhuo G, Bian D (2009) Study on climate feature and grass degeneration on northwest Tibet. *J AL Resour Environ* 23:113–118
- Yin YH, Wu SH, Zheng D, Yang QY (2008) Radiation calibration of FAO56 Penman-Monteith model to estimate reference crop evapotranspiration in China. *Agric Water Manag* 95:77–84
- You YC, Li ZW, Huang C, Zeng H (2017) Spatial-temporal evolution characteristics of land desertification in the Zoige Plateau in 1990–2016. *Ecol Environ* 26:1671–1680
- Yue S, Pilon P, Cavadias G (2002) Power of the Mann-Kendall and Spearman's rho tests for detecting monotonic trends in hydrological series. *J Hydrol* 259:254–271
- Zargar A, Sadiq R, Naser B (2011) A review of drought indices. *Environ Rev* 19(NA): 333–349
- Zhan C, Liang C, Zhao L (2013) Temporal and spatial distribution characteristics and causes analysis of seasonal drought in hilly area of central Sichuan. *Transactions of the Chinese Society of Agricultural Engineering* 29(21):82
- Zhang AZ, Jia GS (2013) Monitoring meteorological drought in semiarid regions using multi-sensor microwave remote sensing data. *Remote Sens Environ* 134:12–23
- Zhang H, Zhang XL, Li JJ, et al. (2018) SPEI-based analysis of temporal and spatial variation characteristics for seasonal drought in Sichuan Basin. *Agricultural Research In The Arid Areas* 36(05):248–256+262
- Zhang XT, Pan XB, Xu L, Wei P, Yin ZW, Shao CX (2017) Analysis of spatio-temporal distribution of drought characteristics based on SPEI in Inner Mongolia during 1960–2015. *Transactions of the CSAE* 33:190–199
- Zhao NN, Gou S, Zhang BB, Yu YL, Han SJ (2017a) Changes in pan evaporation and their attribution to climate factors in the Zoige Alpine Wetland, the eastern edge of the Tibetan Plateau (1969–2014). *Water* 9:971
- Zhao N, Xu MZ, Li ZW, Wang ZY, Zhou HM (2017b) Macroinvertebrate distribution and aquatic ecology in the Ruergai (Zoige) Wetland, the Yellow (IRiver source region. *Front Earth Sci* 11: 554–564
- Zhao GJ, Mu XM, Hörmann G, Fohrer N, Xiong M, Su BD, Li XC (2012) Spatial patterns and temporal variability of dryness/wetness in the Yangtze River Basin. *China Quat Int (in press)* 282:5–13. <https://doi.org/10.1016/j.quaint.2011.10.020>
- Zhao L, Liang C, Cui NB (2013) Attribution analyses of ET0 change in hilly area of central Sichuan in recent 60 years. *J Hydraul Eng* 45: 91–97
- Zhu YL, Chang JX (2017) Application of VIC model based standardized drought index in the Yellow River Basin. *Journal of Northwest A&F University (Nat Sci Ed)* 45:203–212
- Zhuang SW, Zuo HC, Ren PC et al (2013) Application of standardized precipitation evapotranspiration index in China. *Climatic and Environmental Research* 18(5):617–625

**Publisher's note** Springer Nature remains neutral with regard to jurisdictional claims in published maps and institutional affiliations.